

Developmental Efforts of an Electrochemical Oxygen Recovery System for Advanced Life Support

Brittany R. Brown¹, Peter A. Curreri², Ellen M. Rabenberg³,
NASA Marshall Space Flight Center, Huntsville, AL 35812

Jesus A. Dominguez⁴, Lorlyn P. Reidy⁵,
Jacobs JSEG, Huntsville, AL, 35806

Brian Dennis⁶ and Wilaiwan Chanmanee⁷
University of Texas at Arlington, Arlington, Texas, 76019

and

Kenneth A. Burke⁸
NASA Glenn Research Center, Cleveland, Ohio 44135

The current State of Art (SOA) Environmental Control and Life Support System (ECLSS) oxygen recovery system onboard the International Space Station (ISS) is complex, heavy, and power consuming system that recovers approximately 50% of the oxygen (O₂) from metabolic carbon dioxide (CO₂). For future long-duration missions, O₂ recovery systems will need to be highly reliable, efficient, and recover maximum metabolic CO₂. A minimum of 75% O₂ recovery is required for future O₂ recovery systems. Investigations into various technologies to help meet these requirements for exploration are ongoing; however, most of these proposed technologies ultimately result in a more complex system. A Macrofluidic Electrochemical Reactor (MFEER) is one proposed technology development effort currently underway at NASA Marshall Space Flight Center (MSFC) that has the potential to significantly reduce the complexity of ECLSS O₂ recovery system. The MFEER operates at standard conditions, giving it an advantage over other technologies being investigated, which require high temperatures resulting in heavy reactors and high power consumption. The MFEER would replace three pieces of hardware for future ECLSS architectures: the current Carbon Dioxide Reduction Assembly (Sabatier reactor), the Plasma Pyrolysis Assembly (PPA), and the Oxygen Generation Assembly (OGA). It is designed to interface directly with the Carbon Dioxide Removal Assembly (CDRA) and the Water Processor Assembly (WPA). This allows for a less complex system and higher reliability than the current SOA as well as reduced power, weight and H₂O consumption of ECLSS. Here, we will discuss the current technology development efforts of the MFEER and how this technology may aid in the advancement of future long-duration life support systems.

¹ ECLSS Engineer/PI, ECLSS Development Branch, Mail Stop: ES62, MSFC, AL 35812.

² Materials Engineer, Materials Science & Metallurgy Branch, Mail Stop: EM22, MSFC, AL 35812.

³ Materials Engineer, Materials, Test, Chemical & Contamination Control Branch, Mail Stop: EM22, MSFC, AL 35812.

⁴ Electrolysis Engineer, ECLSS Development Branch, Mail Stop: ES62, MSFC, AL 35812.

⁵ Ionic Liquids Chemist, Materials Science & Metallurgy Branch, Mail Stop: EM22, MSFC, AL 35812.

⁶ Associate Professor, Dept. of Mechanical & Aerospace Engineering, 701 S. Nedderman Dr. Arlington, TX 76019.

⁷ Research Associate, Dept. of Mechanical & Aerospace Engineering, 701 S. Nedderman Dr. Arlington, TX 76019..

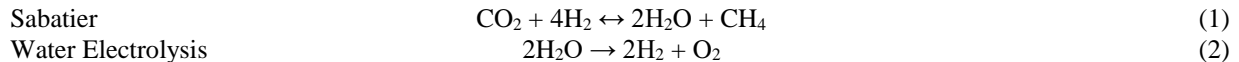
⁸ Electrical Engineer, Photovoltaic & Electrochemical Systems Branch, Mail Stop: LEX0, 21000 Brookpark Rd Cleveland, OH 44135.

Nomenclature

<i>C₂H₂</i>	=	Acetylene
<i>C₂H₄</i>	=	Ethylene
<i>CDRA</i>	=	Carbon Dioxide Removal Assembly
<i>CH₄</i>	=	Methane
<i>CO</i>	=	Carbon monoxide
<i>CO₂</i>	=	Carbon dioxide
<i>CRA</i>	=	Carbon Dioxide Reduction Addembly
<i>Cu</i>	=	Copper
<i>Cu₂O</i>	=	Copper Oxide
<i>CuBr</i>	=	Copper Bromide
<i>ECLSS</i>	=	Environmental Control and Life Support Systems
<i>ISS</i>	=	International Space Station
<i>EORe</i>	=	Electrolytic Oxygen Recovery
<i>Fe</i>	=	Iron
<i>GDE</i>	=	Gas Dffusion Electrode
<i>H₂O</i>	=	Water
<i>IL</i>	=	Ionic Liquid
<i>KOH</i>	=	Potassium hydroxide
<i>MFECR</i>	=	Macrofluidic Electrochemical Reactor
<i>MSFC</i>	=	Marshall Space Flight Center
<i>Ni</i>	=	Nickel
<i>O₂</i>	=	Oxygen
<i>OER</i>	=	Oxygen Evolution Reaction
<i>OGA</i>	=	Oxygen Generation Assembly
<i>PPA</i>	=	Plasma Pyroysis Assembly
<i>Pt</i>	=	Platinum
<i>RT</i>	=	Room Temperature
<i>SEM</i>	=	height
<i>SOA</i>	=	State of the Art
<i>Ti</i>	=	Titanium
<i>UTA</i>	=	University of Texas Arlingotn
<i>WPA</i>	=	Water Processing Assembly

I. Introduction

THE SOA ECLSS Carbon dioxide Reduction Assembly (CRA) is capable of recovering approximately 50% of O₂ from metabolic CO₂. As shown in Equation 1, the CRA consists of a Sabatier reactor which takes in hydrogen (H₂) from the OGA and CO₂ from the CO₂ Removal Assembly (CDRA) and produces water (H₂O) and methane (CH₄.) The CH₄ is vented overboard, and the H₂O is fed to the OGA to produce O₂ and H₂ via H₂O electrolysis (Equation 2). The H₂ is recycled back to the CRA and the O₂ is released into the cabin for crew consumption.



For future long-duration missions, maximum O₂ recovery from metabolic CO₂ is desired. Different technologies that can aid in meeting these requirements are currently being investigated. The current baseline exploration O₂ recovery architecture, shown in Figure 1, encompasses the SOA O₂ recovery system onboard the ISS with the addition of the PPA. The PPA uses a magnetron to generate an H₂/CH₄ plasma that converts the CH₄ generated from Sabatier into mainly H₂ and acetylene (C₂H₂) as shown in Equation 3. Although Sabatier/PPA technology is the current baseline exploration O₂ recovery architecture, alternative approaches, such as the electrolytic reduction of CO₂, may be more desirable technology for future long-duration missions.

In 2016, NASA's Game Changing Development Program awarded the University of Texas Arlington (UTA) a contract to develop a Microfluidic Electrochemical Reactor (MFECR) that has the capability of recovering 73% of

O₂ from metabolic CO₂. This reactor was developed based on the electrochemical reduction of CO₂ to ethylene (C₂H₄) using H₂O as precursor (shown in Equation 4) and operates at ambient pressure and just above the freezing point of H₂O.

PPA
MFECR



The architecture of an Electrolytic O₂ Recovery (EORE) system is shown in Figure 3. The EORE System would reduce the complexity of ECLS Systems (ECLSS) by eliminating the current CRA as well as the PPA and OGA. The current CRA and other technologies that are being investigated (i.e. PPA and Bosch technologies) operate at extremely high temperatures resulting in heavy reactors and higher power consumption making the MFECR highly attractive for future exploration missions.

The MFECR's design, shown in Figure 2, consists of three channels. The two gas channels (anode and cathode) and the electrolyte channel are separated by a Gas Diffusion Electrode (GDE). The GDE surfaces have an electrodeposited layer of nanocomposite particles that act as electro-catalysts for the reaction on the anode and cathode. The electrolyte is a potassium hydroxide (KOH) and H₂O mixture. During the process, KOH is not consumed and therefore does not have to be replaced. However, H₂O is consumed during the process, as illustrated in Equation 4, and needs to be added from the WPA to the KOH-H₂O mixture to replace the consumed water and keep the KOH concentration. To conduct the reactions, an electrical potential is applied on the cathode and the anode GDEs ; O₂ and H₂O are produced on the GDE's anode as hydroxide ion (OH⁻) generated at the GDE's cathode is oxidized, CO₂ consumes H₂O on the GDE's cathode and is

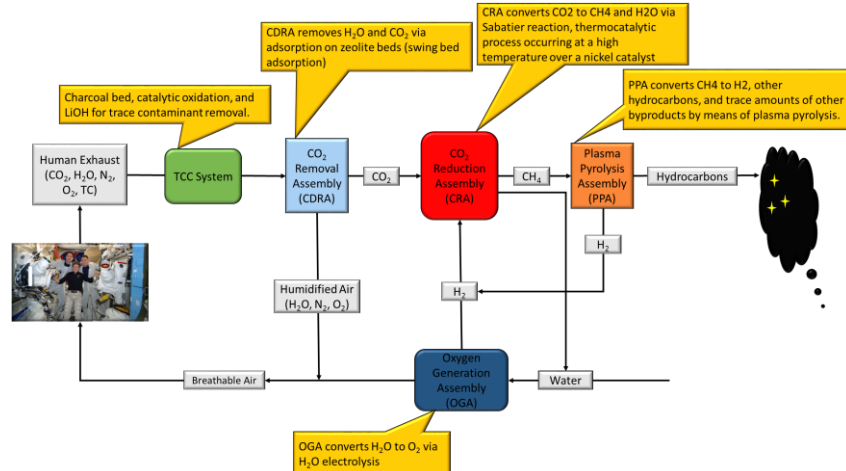


Figure 1. Current SOA O₂ recovery onboard ISS with the addition of PPA.

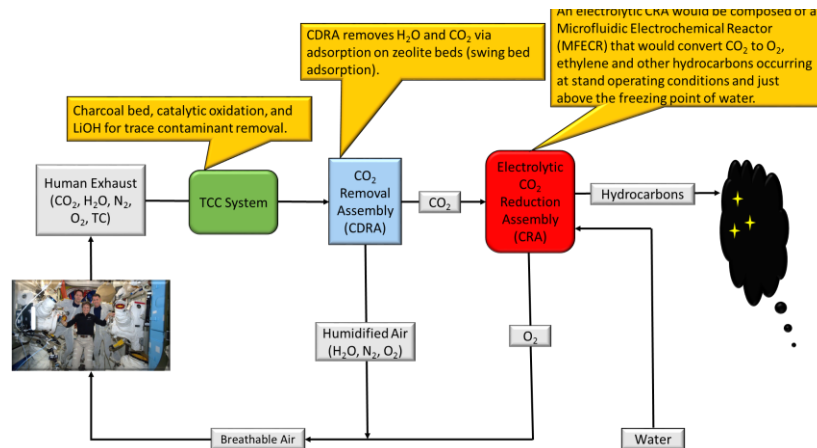


Figure 3. O₂ recovery system for future long duration missions utilizing electrolytic technology, which eliminates the need for OGA, Sabatier, and PPA.

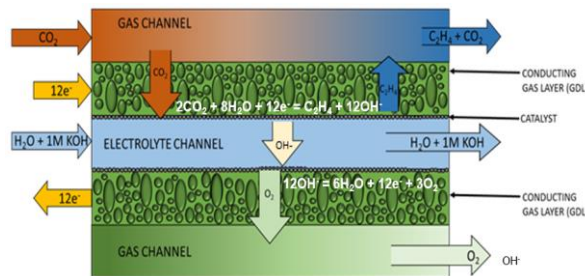


Figure 2. Cross section of the initial design of a single cell MFECR.

reduced generating C_2H_4 and OH . During the process, O_2 and C_2H_4 are produced on opposite sides of the cell, which allows for a gas separation process to be eliminated.

Based on the 2016 developmental efforts by UTA, current NASA collaborative efforts are underway to increase the O_2 recovery efficiency of the process to $>50\%$, advance the technology readiness of the proposed technology to Technology Readiness Level (TRL) 4, and mature the hardware system to process 1.0 kg/day of CO_2 . To achieve these goals, the following improvement areas were identified as pivotal based on initial studies completed by UTA. These improvement areas are discussed in detail in the following sections: anode material development, cathode catalyst development, and optimization of the cell design.

II. Cell Redesign Efforts

A. Alternative Anode Material Selection

Electrochemical conversion of CO_2 involves applying an electrical potential or current between the cathode and the anode to drive the reactions. H_2 and hydrocarbon products are produced in the cathode while O_2 is produced in the anode¹⁻⁵. Overcoming slow kinetics of the Oxygen Evolution Reaction (OER) in the anode requires metal electrodes that exhibit high electrocatalytic activity and require low overpotential. In addition, the anode electrode should be carbon-free to avoid CO_2 formation (commercially available GDEs are equipped with carbon-based GDL) and have a long-term physical and chemical stability in the electrolyte. During initial MFECDR development efforts, the anode showed rapid degradation with time resulting in loss of mechanical strength and conductivity. This ultimately led to leaking of the electrolyte into the O_2 -side gas channel and loss of current density. The development of an alternative anode material is essential for the success of the electrochemical reactor.

Several catalysts such as iridium oxide (IrO_2) and ruthenium oxide (RuO_2) have been studied and are reported to have a high catalytic activity⁶. Recently, hierarchically-structured metal electrodes such as Nickel-Iron (NiFe) foam and Nickel (Ni) foam electrodes have been reported to have even higher catalytic activity owing to their conductivity and high surface area⁷⁻⁹. In this study, several anode materials were evaluated and investigated as electrocatalyst to optimize O_2 production.

1. Experimental

Electrochemical experiments were performed using an open undivided three-electrode cell system using Gamry Instruments Interface 5000E potentiostat/galvanostat. A large surface area platinum (Pt) mesh was used as counter electrode. The reference electrode was $Ag/AgCl$ (4M KCl). Working electrodes that were evaluated for OER were Ni foam, NiFe foam, Ni wire mesh, Pt mesh, and platinized titanium (Ti). Metal electrodes were used as purchased. The surface morphology of the electrodes was evaluated using Scanning Electron Microscopy (SEM) and light microscopy.

Catalytic activity of the anodes was evaluated in aqueous solution 1M KOH electrolyte under argon (Ar) gas blanket. Bulk electrolysis was performed at room-temperature (RT) and at $4^\circ C$ for up to several days. To keep the concentration of 1M KOH constant, the electrochemical cell was designed for flowing electrolyte. A 2-Liter stock solution of 1M KOH was prepared and circulated through the electrochemical cell using a peristaltic pump. H_2O is added into the stock solution to replenish the H_2O lost from electrolysis. For a low-temperature electrolysis, heat exchanger/chiller was used to keep the temperature of the electrolyte and stock solution at $4^\circ C$. The double wall electrochemical cell experimental setup is shown in Figure 4.

For the purpose of this study and the engineering figure of merit for the anode in our microfluidic cell, the calculation of the surface the electrode is simplified to its

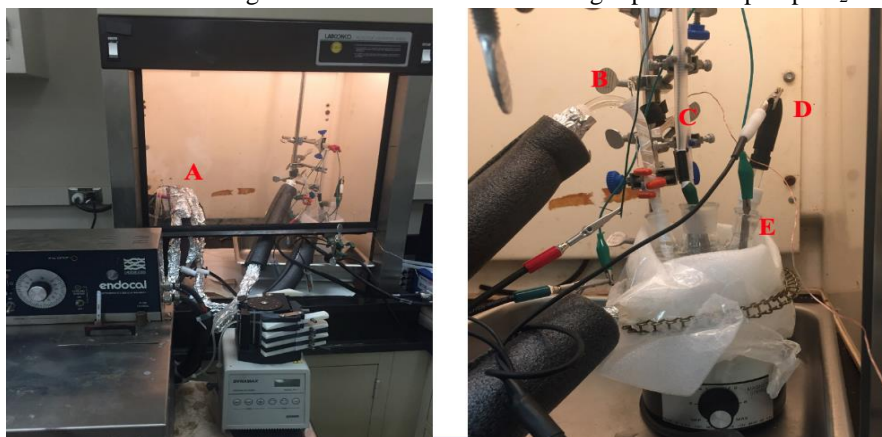


Figure 4. Electrochemical test cell. (A) 1M KOH stock solution chiller system, (B) tubing for circulating 1M KOH , (C) Pt mesh Cathode, (D) $Ag/AgCl$ reference electrode, (E) Ni foam anode.

cross sectional area. Table 1 gives the cross sectional area for the anodes used in this study. Figure 5 SEM or optical micrographs of the morphologies of Platinized Ti Screen, Ni Wire Mesh, Ni-Fe Foam, and Ni Foam respectively.

Table 1. Dimensions and surface area of the cross-section of the anodes that were used as catalyst for the OER measurements.

Electrode	Dimensions (cm)		Surface Area (cm ²)
	Length	Width	
Pt mesh	2.27	1.12	2.53
Platinized titanium replicate 1	0.96	0.94	0.90
Platinized titanium replicate 2	1.39	1.59	2.22
Ni wire mesh	1.42	3.83	5.45
NiFe foam	0.94	1.47	1.38
Ni foam (RT)	1.23	1.47	1.80
Ni Foam (4°C replicate 1)	1.09	1.63	1.77
Ni Foam (4°C replicate 2)	1.14	1.27	1.45

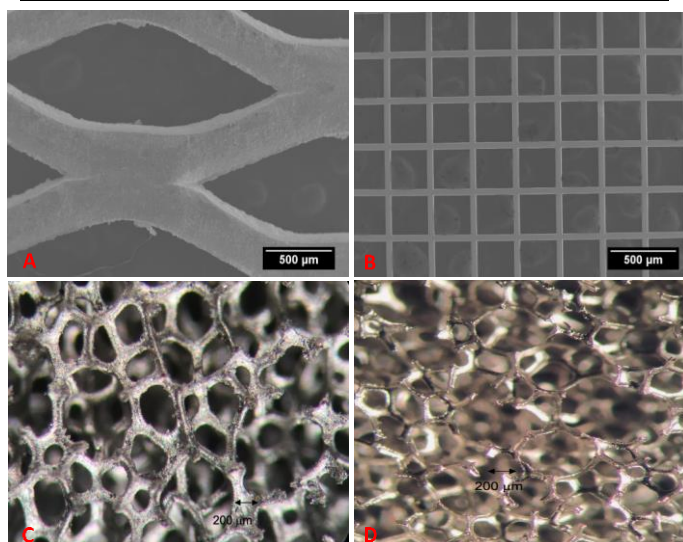


Figure 5. Micrograph using an SEM image of (A) 0.01-inch thick Platinized Ti Screen, (B) 80x80 Ni wire mesh, (C) 2mm thick Ni-Fe foam with atomic ratio of 3:1. (D) Micrograph of 1.4 mm thick Ni foam using light microscopy.

2. Results and Discussion

Electrocatalytic activity and stability of the anode electrodes were evaluated using chronoamperometry. The current density of the electrodes were measured as a function of time. Chronoamperometric measurements of OER at the anode were performed using 1M KOH at an applied potential of 3V vs Ag/AgCl. Bulk electrolysis was conducted at RT for up to several days. OER activity and stability of the Ni foam were also evaluated at lower temperature, 4°C, which may be more optimum for the MFECDR application.

NiFe foam gave better current density than the platinum mesh electrode. However, the current density decreases over time and the electrolyte slowly changed from a clear solution to yellowish in color. This suggests that some iron (Fe) could be dissolved and introduced into the electrolyte. Platinized Ti showed poor stability and OER performance, due to the loss of catalytic activity over time. This may suggest that the passivation from the Pt coating was not complete.

The anodic chronoamperometric scans on the electrodes are summarized on Figure 6. The Ni foam anode gave the best catalytic performance among the electrodes that were evaluated at RT, since it gave the highest current density. Ni did not dissolve and the anodes were mechanically stable. The absence of dissolved Ni ions in the electrolyte was confirmed by elemental analysis using Inductively Coupled Plasma-Mass Spectrometry (ICP-MS). The catalytic

performance of the Ni foam electrode may be attributed to its high surface area and porous structure which is found to be effective in dissipating O₂ bubbles⁸. The optical micrograph of Ni foam electrode is shown in Figure 5. The OER activity and stability of the Ni foam anode evaluated at lower temperature, 4°C is given in Figure 7. The temperature stability is given in Figure 8. The current density at 4°C was significantly lower but it remained stable over 3 days of electrolysis.

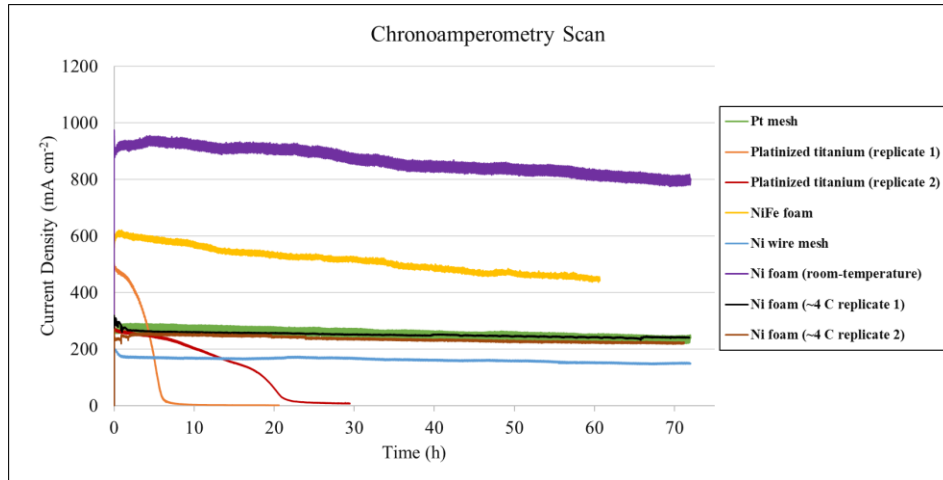


Figure 6. Chronoamperometric measurements of OER at various anodes: Ni wire mesh (blue), platinized Ti (red and orange), and NiFe foam (yellow), Ni foam (purple, brown and black), and Pt mesh (green). OER tests were evaluated using 1M KOH at RT and at 4°C.

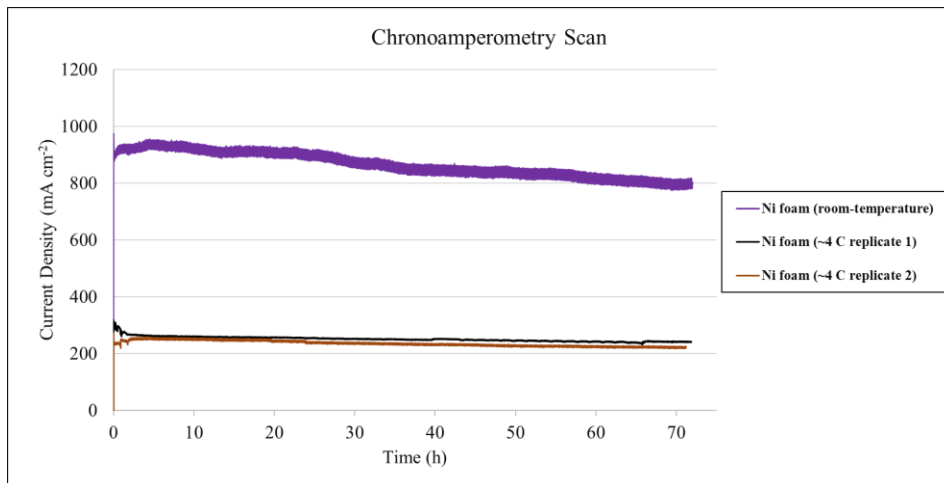


Figure 7. Chronoamperometric measurements of OER at best performing Ni Foam anode using 1M KOH at room temperature and 4°C.

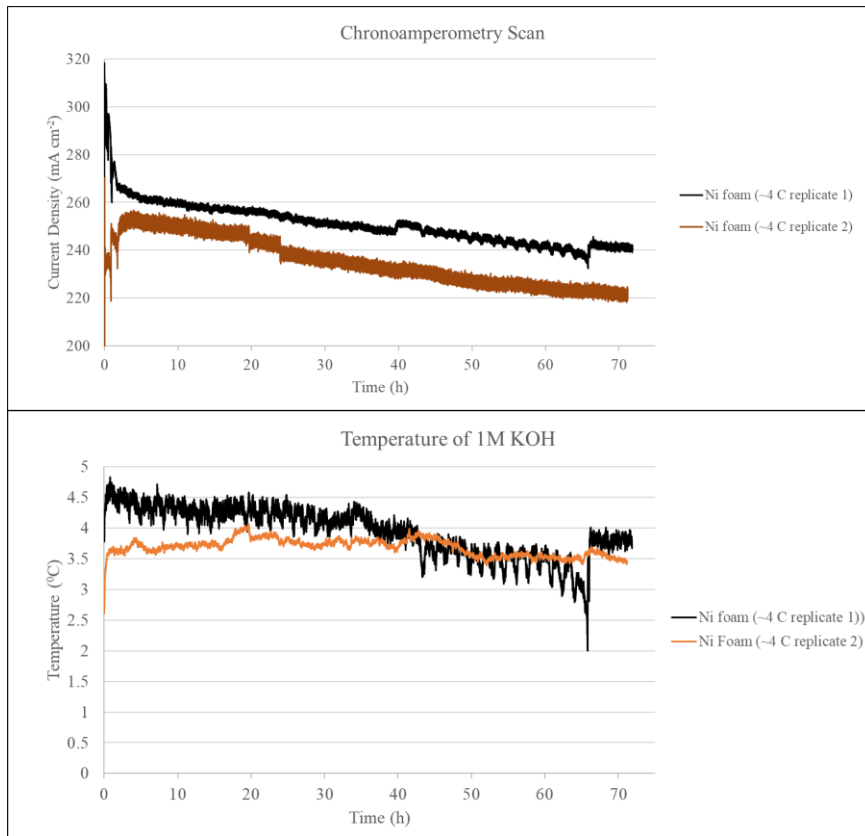


Figure 8. (Top) OER at Ni in 1M KOH, (Bottom) corresponding temperature of 1M KOH during OER.

B. Alternative Electrolyte Solution Selection

The choice for the electrolyte in the electroreduction of CO₂ is important to optimize the production of O₂. The baseline electrolyte for the MFECD system is 1M KOH. KOH provides good conductivity, optimum pH, while providing good materials compatibility for the selected electrodes. However, KOH poses a spill and corrosion hazard in a spacecraft environment and may not be an optimum absorber for CO₂ gas.

There has been a rising interest on the use of ionic liquid (IL) as an electrolyte for CO₂ capture and electrochemical processing.¹⁻⁵ ILs are organic salts that are composed entirely of ions and exist as liquid below 100°C. They have high thermal stability and negligible vapor pressure. ILs are tunable and can be designed to be task-specific for chemisorption or physisorption of CO₂ gas. Some ILs have high affinity and solubility for CO₂. These unique properties of IL make it an attractive alternative for the baseline alkaline KOH solution. In this study, preliminary investigations on the use of IL as electrolyte for MFECD were conducted.

1. Experimental

The ILs evaluated along with their solubility and electrode materials compatibility are listed in Table 1. [EMIm][CF₃Pyra], [P₄₄₄₁₄][CNPyrr], and [DABCO][CF₃Pyra] were synthesized in-house. [BuMePyrr][DCA] was used as purchased from Sigma Aldrich. The rest of the ILs listed in Table 1 were purchased from Io-Li-Tec without further treatments. The ILs were evaluated based on its solubility in H₂O, compatibility with Ni and copper (Cu) metal electrodes, and current efficiency in OER. The catalytic activity of the Ni foam anode in the IL electrolyte is compared to that of the baseline electrolyte, 1M KOH solution.

Electrochemical experiments were performed using an open undivided three-electrode cell system using Gamry Instruments Interface 5000E potentiostat/galvanostat. The counter electrode was a large surface area Cu foam cathode and the reference electrode was Ag/AgCl (4M KCl). Ni foam anode was used as the working electrode. The current efficiency of these electrolytes were evaluated by bulk electrolysis using Cu foam cathode and Ni foam anode. CO₂ gas is constantly bubbling through the solution during the duration of the electrolysis. The surface area of the anode

was simplified and calculated based on the cross-section of the electrode. Chronoamperometric measurements of the OER were performed at RT using an applied potential of 2.0V vs Ag/AgCl.

CO₂ gas is constantly bubbling through the solution during the duration of the electrolysis. The surface area of the anode was simplified and calculated based on the cross-section of the electrode. Chronoamperometric measurements of the OER were performed at RT using an applied potential of 2.0V vs Ag/AgCl.

Table 1. IL electrolytes that were evaluated for solubility in H₂O and compatibility with Ni and Cu electrodes

Electrolyte Name	Electrolyte Abbreviation	Solubility in H ₂ O	Compatibility with Cu	Compatibility with Ni
1-ethyl-3-methylimidazolium acetate	[EMIm][OAc]	soluble	Reacted with Cu; solution turned blue	Compatible
1-Butyl-3-methyl-imidazolium acetate	[BMIm][OAc]	soluble	Reacted with Cu; solution turned blue	Compatible
1-ethyl-3-methylimidazolium triflate	[EMIm][TFO]	soluble	Solution turned pale green	Compatible
1-Butyl-3-methyl-imidazolium triflate	[BMIm][TFO]	soluble	Compatible	Compatible
1-Butyl-1-methylpyrrolidinium triflate	[BuMePyr][TFO]	soluble	Compatible	Compatible
1-ethyl-3-methylimidazolium ethylsulfate	[EMIm][Ethylsulfate]	soluble	Solution turned pale green	Compatible
1-Butyl-1-methylpyrrolidinium dicyanamide	[BuMePyr][DCA]	soluble	Solution turned green and black precipitate is observed in the solution	Compatible
1-ethyl-3-methylimidazolium bis(trifluoromethylsulfonyl)imide	[EMIm][TFSI]	not soluble		
1-Butyl-3-methyl-imidazolium bis(trifluoromethylsulfonyl)imide	[BMIm][TFSI]	not soluble		
1-Butyl-1-methylpyrrolidinium bis(trifluoromethylsulfonyl)imide	[BuMePyr][TFSI]	not soluble		
1-ethyl-3-methylimidazolium 3-trifluoromethyl-pyrazolide	[EMIm][CF ₃ Pyra]	not soluble		
Tributyltetradecylphosphonium 2-cyanopyrrolide anion	[P ₄₄₄₁₄][CNPyr]	not soluble		
1,4-diazabicyclo[2.2.2]octane 3-trifluoromethyl-pyrazolide	[DABCO][CF ₃ Pyra]	not soluble		

2. Results and Discussion

The reaction mechanism for the electrochemical reduction of CO₂ requires H₂O as precursor of H₂ for the production of C₂H₄ in the cathode. Thus, the IL has to be soluble in H₂O. The ILs, [EMIm][OAc], [BMIm][OAc], [EMIm][TFO], [BMIm][TFO], [BuMePyr][TFO], [EMIm][Ethylsulfate], [BuMePyr][DCA] were H₂O soluble and further tested for compatibility with Cu and Ni metal electrodes. Of the ILs evaluated in this study, [BMIm][TFO] and [BuMePyr][TFO] met the criteria needed for the MFECR as shown above in Table 1.

Bulk electrolysis and chronoamperometric evaluations of the OER at the Ni foam anode on the 1M aqueous solution of [BuMePyr][TFO] and 1M KOH aqueous solution were performed. Comparison on the anodic current density between the two electrolytes are shown in Figure 9. The current density for oxygen production is higher in the KOH than in the [BuMePyr][TFO].

Of the twelve ILs investigated as an alternative electrolyte for MFECR, two were found to be soluble in H₂O and compatible with Ni and Cu electrode materials. The IL [BuMePyr][TFO] was evaluated and compared against the baseline electrolyte, 1M KOH. [BuMePyr][TFO] was determined to be a candidate alternate electrolyte for the MFECR process, but the OER activity of Ni foam anode in KOH is still superior to [BuMePyr][TFO]. However, [BuMePyr][TFO] can be tested in the MFECR apparatus for CO₂ absorption and overall system efficiency. Additional testing of the other compatible candidate, [BMIm][TFO], is planned. Additional efforts to continue the

search and evaluation of alternative electrolytes for an optimum alternative electrolyte for the electroreduction of CO₂ will be made.

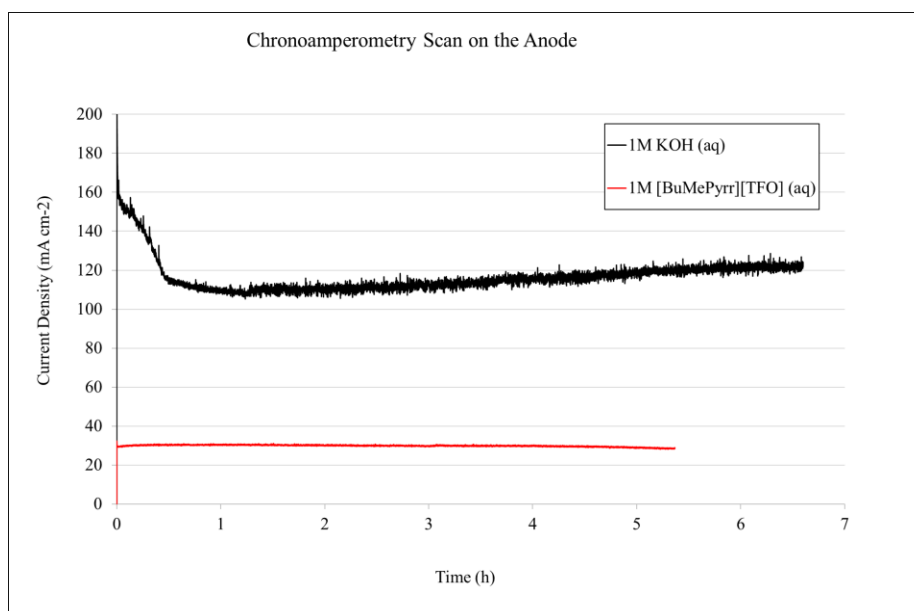


Figure 9. Chronoamperometric measurements of OER at a Ni foam anode using 1M KOH and 1M [BuMePyrr][TFO] as electrolyte.

C. Cathode Catalyst Optimization

Traditional metal electrodes for CO₂ electrochemical reduction have problems with CO₂ conversion to CO instead of conversion to useful hydrocarbons, as well as issues with rapid decrease in CO₂ reduction within tens of minutes during electrolysis. During initial MFECR development efforts, UTA developed a cathode composed of electrodeposited copper oxide (Cu₂O) – copper bromide (CuBr) films on the GDL side of the GDE, as shown in Figure

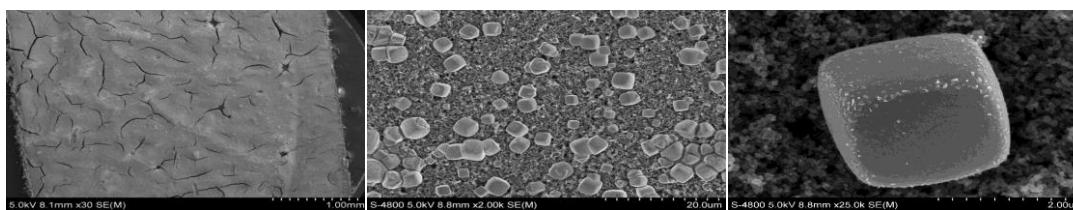


Figure 10. Representative SEM images of hybrid Cu₂O-CuBr films electrodeposited on GDL 35BC, whose unique morphology is shown to be the key to effectiveness of the technology

10, which enhances CO₂ conversion to mainly C₂H₄ and generates H₂ during the process.¹⁴ Current efforts are focused on further development of the advanced cathode catalyst due to the observance of a shift in selectivity towards hydrocarbons due to the compositional changes in the cathode electro-catalyst with time.

Although the electrochemical deposition method for producing the cathode catalyst on GDL, little effort was focused on optimizing larger diameter GDLs that are needed for larger scale testing. A new deposition reactor, shown in Figure 11, was developed at UTA for larger GDLs that includes stirring of the electrolyte and horizontal orientation in an effort to make the deposition

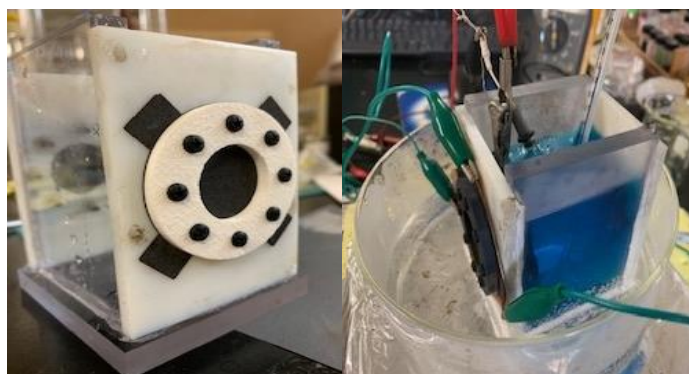


Figure 11. The new deposition reactor includes stirring of the electrolyte and horizontal orientation to make a universal deposition layer across the GDL.

layer uniform across the GDL. A conductive backing that contacts the back of the GDL was used to create a more uniform current distribution.

1. Experimental

The cathode GDL that was fabricated in the new deposition reactor was tested in a single cell microreactor. The Computer Aided Design (CAD) model and 3D printed reactor test setup is shown in Figure 12. The fabricated cathode in the new deposition reactor and high purity Ni foam was used as the anode during testing. The electrolyte was 1 M KOH at 10-15 °C with flow rate of 10 mL/min. CO₂ gas was continuously flowing at 5 mL/min through the back of GDL supporting electrode which was covered by the Cu₂O-CuBr. A voltage of -4V was applied to the cell and a gas chromatography (GC) instrument was used to analyze the composition of product formation .on the outlet at the back of the cathode GDL.

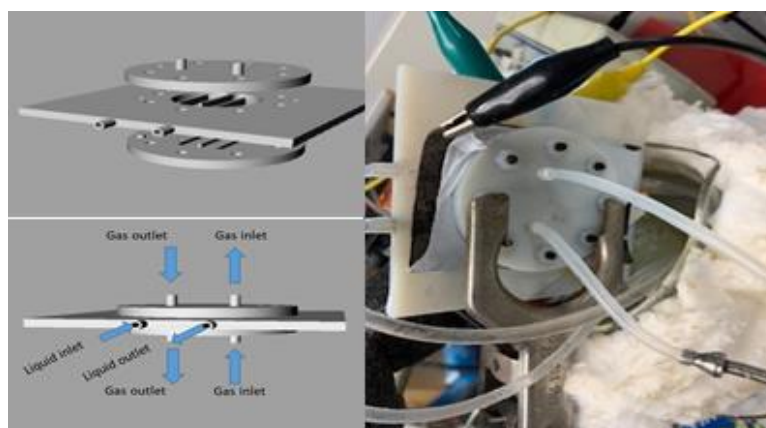


Figure 12. (A) CAD model of the microreactor. (B) 3D printed

2. Results and Discussion

The results of testing are shown in Figure 13. During ten hours of CO₂ electroreduction, the GC detected C₂H₄, H₂, and CH₄ in the gas products. However, there is an observance of decreasing current and increasing H₂ formation as time progresses. This current decrease is sensing changes at the cathode and/or anode surface where the surface becomes less accessible to CO₂ molecules.

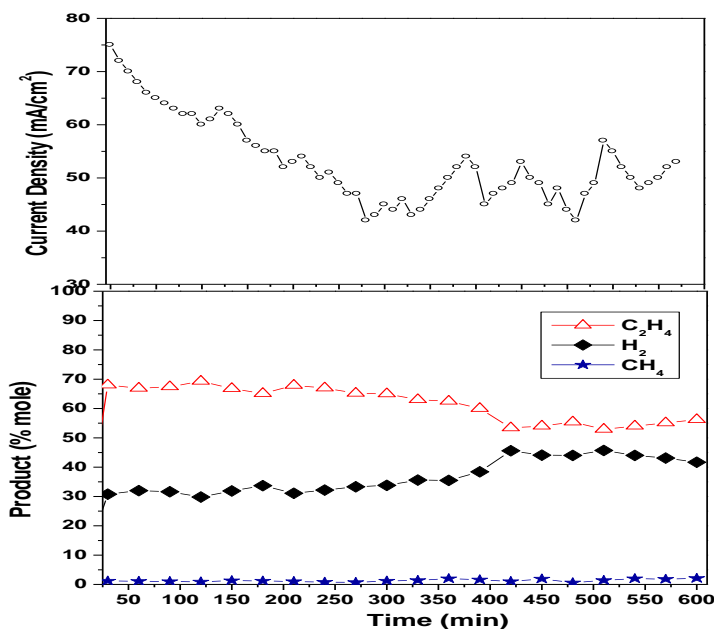


Figure 13. Current/time profiles at -4V for Cu₂O-CuBr film on GDL in microreactor.

D. Optimization of Cell Design

In order to increase the conversion rate of the MFECR, further optimization of the cell design was investigated. During initial development efforts, the original serpentine design during small scale testing showed great promise with a 54% metabolic CO₂ conversion rate. Efforts to scale the design ultimately led to a design modification, shown in Figure 14, due to manufacturing issues with the designs thin channel walls. Current efforts were made to fabricate the serpentine design using alternative machining capabilities, such as laser cutting. The successful fabrication of a serpentine electrode is shown in Figure 15. Alternative materials, shown in Table 2, were chosen to be investigated in order to optimize the MFECR. Various thicknesses and each material will be investigated to determine optimal performance with the goal, if possible, to minimize weight and volume of the cell stack. The original endplates of the cell design were composed of stainless steel plates, which are conductive. The non-conductive properties of polyester and polycarbonate will result in lower potential loss. However, the key here is stiffness. Non-metals are not as stiff as metals, which result in thicker endplates. For the current distributor, nickel alloy and cobalt-infused (POCO) graphite will be investigated instead of pure graphite to avoid degradation due to oxidation. The non-conductive/corrosive properties of Teflon instead of graphite was chosen to avoid degradation due to oxidation and loss of potential. The fully assembled MFECR, shown in Figure 16, will be installed into the test stand and evacuated once fabrication of the test stand is complete.

Additional efforts are being made to optimize design and operation of the MFECR with the development of a comprehensive 3D multi-physics model. The test stand will provide all the instrumentation and sensors required to fully validate the model. The MFECR 3D multi-physics model effort is detail in “Modeling Electrolytic Conversion of Metabolic CO₂ and Optimizing a Microfluidic Electrochemical Reactor for Advanced Closed Loop Life Support Systems”.¹⁵

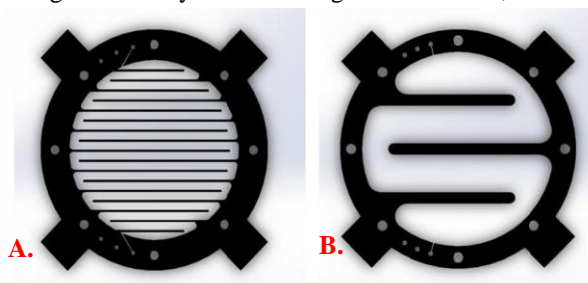


Figure 14. Design modification made from the original serpentine design (A) to the wider channel design (B).

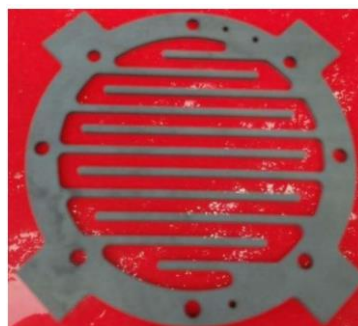


Figure 15. Successful fabrication via laser jet of an electrode.



Figure 16. Fully assembled MFECR.

Table 2. Alternative material selections of components for optimization of the MFECR.

MFECR Component	Original Design Material Selection	Redesign Material Selection
Endplate	Stainless Steel	Polyester
		Polycarbonate
Current Distributor	Graphite	Nickel Alloy
		POCO Graphite
Electrolyte Wall	Graphite	Teflon

III. Conclusion

The development of a MFECR that has the capability of recovering 73% of O₂ from metabolic CO₂ at ambient conditions is currently under development. Optimizations of the original MFECR design include the development of an alternative anode material due to rapid degradation with time resulting in loss of mechanical strength and conductivity. Several anode materials were investigated, and based on the results, Ni foam was chosen as the anode material of choice. Alternative electrolyte solutions have been investigated due to the corrosive properties of KOH. Several IL electrolytes were investigated, and although some ILs look promising, none have been selected as a feasible alternative to KOH. The cathode catalyst advancement is an ongoing effort to maximize C₂H₄ production and minimize H₂ production during the process. Alternative materials have been chosen for the MFECR design and will be tested in the near future at MSFC to determine optimal material selection for the final MFECR design.

Acknowledgments

The authors would like to thank Max McCall for mechanical design, Wes Shelton for technician support, Tom Williams for software support. The authors would like to also thank all the interns who have supported this effort: Allison Burns, Michael Veksler, Matthew Russell, and Samantha Hall.

References

- ¹ Abney, M.B., Karr, L.J., Paley, M.S., Donovan, D.N., Kramer, T.J., "Life Support Catalyst Regeneration Using Ionic Liquids and In Situ Resources," 46th International Conference on Environmental Systems, Vienna, Austria, July 10-14, 2016.
- ² Brown, B.R., Fox, E.T., Karr, L.J., Stanley, C., Abney, M., Donovan, D.N., Paley, M.S., McLeroy, J.L., "Utilizing Ionic Liquids to Enable the Future of Closed-Loop Life Support Technology," *48th International Conference on Environmental Systems*, ICES-2018, Albuquerque, New Mexico, 2018.
- ³ Masato Sakuai, Asuka Shima, Kazuyuki Iwasaki, Yoshiyuki Sometani, Takuya Goto, Yasuhiro Fukunaka and Mitsuhiro Kanakubo, "Preliminary Study of CO₂ electrolysis in Ionic Liquid", Proc. 49th International Conference on Environmental systems, ICES-2019-141 (2019)
- ⁴ Michael Manning, "An Investigation of the Bosch Process", Massachusetts Institute of Technology Dissertation, 1976
- ⁵ Manuel Alvarez-Guerra, Jonathan Albo, Enrique Alvarez-Guerra, and Angel Irabien, "Ionic Liquids in the Electrochemical valorization of CO₂", *Energy Environ. Sci.*, 8 (2015) 2574-2599
- ⁶ Charles McCrory, Suho Jung, Jonas Peters, and Thomas Jaramillo, "Benchmarking Heterogeneous Electrocatalyst for the Oxygen Evolution Reaction", *J. Am. Chem. Soc.* (2013), 135, 45, 16977-16987
- ⁷ Yanhui Liang, Qian Liu, Abdulla M. Asiri, Zuping Sun, and Yaquan He, "Nickel-iron foam as a three-dimensional robust oxygen evolution electrode with high activity." *International Journal of Hydrogen Energy* 49 (2015) 13258-13263.
- ⁸ Xunyu Lu and Chuan Zhao, "Electrodeposition of hierarchically structured three-dimensional nickel-iron electrodes for efficient oxygen evolution at high current densities," *Nature Communications* 6.6616 DOI 10.1038/www.nature.com/naturecommunications, pg. 1-7.
- ⁹ Peili Zhang, Lin Li, Dennis Nordlund, Hong Chen Lizhou Fan, biaobiao Zhang, Xia Shen, Quentin Daniel, and Licheng Sun, "Dendritic core-shell nickel-iron-copper metal/metal oxide electrode for efficient electrocatalytic water oxidation," *Nature Communications* (2018) 9.381, DOI: 10.1038/s41467-017-02429-9, www.nature.com/naturecommunications, pgs. 1-10.
- ¹⁰ Samuel Seo, Mauricio Quiroz-Guzman, M. Aruni DeSilva, Tae Bum Lee, Yong Huang, Brett Goodrich, Williaam Schneidr, and Joan Brennecke. Chemically Tunable Ionic Liquids with Aprotic Heterocyclic Anion (AHA) for CO₂ Capture. *J. Phys. Chem. B* 2014, 118, 5740-5751
- ¹¹ Manuel Alvarez-Guerra, Jonathan Albo, Enrique Alvarez-Guerra, and Angel Irabien, Ionic Liquids in the Electrocheical Valorisation of CO₂, *Energy Environ. Sci.* 2015, 8, 2574-2599
- ¹² Masato Sakuai, Asuka Shima, Kazuyuki Iwasaki, Yoshiyuki Sometani, Takuya Goto, Yasuhiro Fukunaka and Mitsuhiro Kanakubo, "Preliminary Study of CO₂ electrolysis in Ionic Liquid", Proc. 49th International Conference on Environmental systems, ICES-2019-141 (2019)
- ¹³ David Grills, Yasuo Matsubara, Yutaka Kuwahara, Suzzane Goliz, Daniel Kurtz, and Barbara Mello. Electrocatalytic CO₂ Reduction with a Homogeneous Catalyst in Ionic Liquid: High Catalytic Activity at Lower Overpotential. *J. Phys. Chem. Lett.* 2014, 5, 2033-2038
- ¹⁴ Tacconia N. R., Chanmanee W., Dennis B., Rajeshwarb K., Composite copper oxide-copper bromide films for the selective electroreduction of carbon dioxide, *J. Mater. Res.*, Vol. 32, No. 9, May 15, 2017; pp. 1727-1724
- ¹⁵ Dominguez, J., Brown, B., Reidy, L., Curreri, P., Rabenberg, E., Dennis, B., Chanmanee, W., Burke, K., "Modeling Electrolytic Conversion of Metabolic CO₂ and Optimizing a Microfluidic Electrochemical Reactor for Advanced Closed Loop Life Support Systems," 50th International Conference on Environmental Systems, Lisbon, Portugal, July 12-16, 2020.